Biosensors and Bioelectronics 135 (2019) 45–49

Contents lists available at ScienceDirect

Biosensors and Bioelectronics

journal homepage: www.elsevier.com/locate/bios

Enzyme-free glucose sensor based on layer-by-layer electrodeposition of multilayer films of multi-walled carbon nanotubes and Cu-based metal framework modified glassy carbon electrode

Lan Wu, Zhiwei Lu*, Jianshan Ye**

College of Chemistry and Chemical Engineering, South China University of Technology, Guangzhou, 510641, PR China

ARTICLE INFO

Keywords:
Nonenzymatic glucose sensor
Electrodeposition
Multilayer films
Cu-MOF/MWNTs/GCE

ABSTRACT

A high-performance nonenzymatic glucose sensor was successfully prepared by a layer by layer strategy through electrodeposition assembling multilayer films of Cu-metal-organic frameworks/multi-walled carbon nanotubes (Cu-MOF/MWNTs) modified glassy carbon electrodes (GCE). Different multilayer films of Cu-MOF/MWNTs modified GCE (Cu-MOF/MWNTs/GCE) were prepared by repeating the electrodeposition of MWNTs onto the GCE in an MWNTs solution (MWNTs/GCE) and electrodeposition of the Cu-MOF layer onto the MWNTs film surface to form a Cu-MOF/MWNTs composite layer in the crystallization solution of Cu-MOF. Results confirmed that this method to fabricate multilayer composite films on the GCE was fast and convenient, and that multilayer composite films were stable and unified. The electrode modified by the multilayer composite films could effectively increase the exposure of active sites and increase the surface area of reactive contact. The GCE modified by eight layers (four multilayers Cu-MOF/MWNTs films) showed the optimum catalytic performance in the oxidation of glucose. The novel glucose sensor exhibited a wider detection linear range of 0.5 μM–11.84 mM, with a detection limit of 0.4 μM and a sensitivity of 3878 μA cm^{-2} mM^{-1}. Moreover, the electrochemical response of the sensor on glucose was fast (within 0.3 s) and stable, exhibited good selectivity and was free of interference.

1. Introduction

In the catalytic analysis of chemistry, materials and other disciplines, how to improve the catalytic performance to achieve the maximum catalytic effect largely depends on the quality of modified electrodes, that is, the modification of solid substrate (Kang et al., 2012). The most common modification method is loading coating, which means that synthetic materials with good catalytic effects are fixed to the solid substrate surface by certain actions, such as adsorption, electrodeposition and adhesives adhesion (Luo and Epps, 2013). Among the many modified materials with high selectivity catalysis, metal-organic framework (MOF) represents a new type of porous 3D mesh material that has recently attracted considerable attention (Morris et al., 2012a; Tranchemontagne et al., 2009). MOF has porous structures with a high specific surface area through the coordination between metal ions and different organic ligands and realize structure and pore size regulation (Ji et al., 2018). HKUST-1 is one of the MOF formed with copper (Cu) atoms as the center and with carboxylic acid ligands (1,3,5-benzenetricarboxylic acid) as coordinators. When heated, water molecules can be easily removed to acidify the central Cu. Meanwhile, reactants can react with the central Cu through the pores, thereby catalyzing the reaction. MOFs are considered and applied as a type of developed sensor. However, MOF materials are limited in application because of their poor conductivity and restricted catalytic properties. Therefore, the current approach to enhancing the performance of MOF is to combine them with nanocarbon materials to form multi-element composite materials. A good choice of nanocarbon material is the carbon nanotube (CNT) because of its excellent physical properties and high content of carboxyl groups and other functional groups after nitrification treatment; these groups can immobilize with other materials through an electrostatic action (Kim et al., 2014) or bond cooperation (Yun S, 2009).

Recently, the new synthesis strategy of Cu-MOF composite materials and the application in modifying electrodes have become a research focus. As early in 2007, researchers have found that the growth of the Cu-MOF can be controlled by directional self-assembled monolayers

* Corresponding author. School of Chemistry and Chemical Engineering, South China University of Technology, Guangzhou, 510641, PR China.
** Corresponding author. School of Chemistry and Chemical Engineering, South China University of Technology, Guangzhou, 510641, PR China.
E-mail addresses: luzhiwei514@163.com (Z. Lu), jsye@scut.edu.cn (J. Ye).

https://doi.org/10.1016/j.bios.2019.03.064
Received 20 January 2019; Received in revised form 22 March 2019; Accepted 31 March 2019
Available online 09 April 2019
0956-5663/

(SAMs) with varying functionalization. However, this technique requires available appropriate functional groups on surfaces, such as -COOH and -OH (Biemmi et al., 2007). Referring to previous studies, Yanli Zhou et al. successfully prepared high-density cross-linked copper framework thin films by in situ growth of sheet structure Cu-MOF on graphene functionalized SAMs on gold substrates electrodes (Zhou et al., 2018). Liudi Ji (Ji et al., 2018) provided an electrochemical method for the rapid and simple synthesis of MOF using crystal mother liquor at a certain voltage. The MOF synthesized by this method exhibits distinct properties and structural stability. Based on this factors, Cu-based MOF materials achieve a satisfactory catalytic oxidation effect on glucose. Shi et al. (2016) encapsulated Cu nanoparticles in ZIF-8 to form Cu-in-ZIF-8 as a sensitive nonenzymatic glucose sensor, which was attributed to the synergistic of Cu nanoparticles with small particle size and ZIF-8 with porous structure. In addition, biomolecules combined with MOF have been used for biosensing to catalyze glucose. For example, He et al. (2016) prepared Cu-hemin-MOF with glucose oxidase (GOD) for electrochemical detection of glucose. Liu et al. (2016) applied HKUST-1 MOF as a porous matrix to encapsulate hemin to form Hemin@HKUST-1 composites for H_2O_2 and glucose detection by chemiluminescence method. Therefore, using new non-traditional synthetic MOF materials to build highly effective glucose sensors is an important research topic. Glucose, is an important indicator of human health, and is directly related to the normal operation of other systems. Therefore, how to timely and effectively determine the level of glucose or blood glucose is of great significance for clinical practice and other fields. Traditional glucose detection methods require long testing time, complicated large instruments, poor selectivity. So, good selectivity, high sensitivity, fast response time of the electrochemical methods have become a research hot spot.

On the basis of the abovementioned considerations and factors, for the first time in this present study, Cu-MOF crystallization solution and MWNTs solution were electrodeposited on the glassy carbon electrode several times to form a multilayer film of Cu-MOF/MWNTs non-enzymatic glucose sensor. This provides an effective and promising method for the preparation of highly efficient and sensitive non-enzymatic glucose sensors.

2. Experimental section

On the basis of the previous literature, Cu-MOF was obtained by hydrothermal synthesis based, and MWNTs were carboxylated. Specific experimental materials, characterization methods, and synthesis processes can be found in the Supporting Information.

2.1. Multilayer film preparation

The synthesis strategy of Cu-MOF and multilayer films of Cu-MOF/MWNTs/GCE are briefly illustrated in Scheme 1 according to the following steps: (additional details in Supporting Information).

Step One The GCE was polished with alumina powder and sonicated for 2 min in ethanol and ultrapure water, and then immersed in MWNTs solution under the deposition voltage of −1.3 V for 200 s. The resulting MWNTs/GCE was pulled out and washed with ultrapure water.

Step Two The prepared MWNTs/GCE was immersed into the prepared Cu-MOF crystallization solution at 1.7 V and electrodeposited for 200 s, forming one Cu-MOF/MWNTs layer. Then Cu-MOF/MWNTs/GCE was taken out and washed with ultrapure water.

Step Three The different layers of multilayer films modified GCE was assembled by repeating step one and two several times until the deposition of multilayer films of Cu-MOF/MWNTs/GCE was completed.

3. Results and discussion

3.1. Characterization of Cu-MOF, MWNTs, and multilayer films of Cu-MOF/MWNTs/GCE

To facilitate subsequent characterization, the material was electrodeposited on a conductive diamond wafer for scanning electron microscope (SEM) determination (Fig. 1a). As shown in Fig. 1b, the MWNTs films completely covered the surface of diamond substrates and were uniformly distributed without agglomeration with large membrane holes appear in the gap. After the deposition of Cu-MOF, most of MWNTs is covered below (Fig. 1d). Crystal particles with distinct edges and angles were deposited on the surface, successfully indicating that the Cu-MOF were completely deposited on the MWNTs-modified substrate. As sedimentary layers increased in number, the growth of MWNTs and Cu-MOF showed a certain increase aggregation, MWNTs and Cu-MOF aggregated separately and intertwined at the ends.

The crystallinity and phase purity of the electrodeposited Cu-MOF were clarified using XRD (Fig. S2a). The XRD pattern of the sample is consistent with that in the literature (Chowdhury et al., 2009; Ji et al., 2018; Morris et al., 2012b). XPS (Fig. S2b) was also used to characterize the surface composition information. As shown in Fig. S2c of C 1S, the peak positions were noted at 284.4, 287.3, and 288.7 eV, which are respectively attributed to graphite carbon, C-O-C, and O-C=O (Ali Khan et al., 2014; Okpalugo et al., 2005). The Cu 2p spectrum (Fig. S2d) showed two characteristic peaks at 932.4 and 952.2 eV, corresponding to $2p_{3/2}$ and $2p_{1/2}$ of metallic Cu, respectively. At approximately 943 eV, weak peaks were observed, and they were attributed to the satellite peak of Cu^{2+}.(Ji et al., 2018; Maruyama, 1998). In addition, FT-IR results shown that the MWNTs-COOH treated with nitrification successfully connected to carboxyl and other activity groups (detailed discussion is available in the Supporting Information).

3.2. Electrocatalytic behavior of the modified electrodes

As presented in Fig. 2a, the cyclic voltammogram (CV) curves of bare GCE, MWNTs/GCE and Cu-MOF/MWNTs/GCE in KCl solution containing 5 mM $[Fe(CN)_6]^{3-/4-}$ were compared. The CV curve of bare GCE presented a significant pair of anodic and cathodic peaks. After MWNTs-COOH electrodeposition, the CV curve largely decreased relative to the curve of the GCE. The deposited MWNTs comprised a multitude of negatively charged groups, such as –COOH, after being carboxylated, thereby causing the MWNTs to repel the negative redox probe in the solution and reduce the electron conduction. After electrodeposition of Cu-MOF, the CV curve showed a pair of typical electrochemical response peaks of Cu ion conversion from Cu (II) to Cu (I).

Nyquist plots (Fig. 2b) of the different modified electrodes were obtained at an open-circuit voltage by using the frequency range of 1 Hz–100 kHz. The bare GCE exhibited a relatively small R_{ct} of approximately 113 Ω. However, after the electrodeposition of the MWNTs, R_{ct} expanded to approximately 171 Ω because of the abundant carboxyl groups on the MWNTs surface that impeded the electron transfer of $[Fe(CN)_6]^{3-/4-}$. When electrodeposited with layers of MWNTs and Cu-MOF, R_{ct} notably increased at approximately 1.317 kΩ because the Cu-MOF acted as a barrier and an interfacial electron transfer blocking layer that greatly attenuated the electron transfer of $[Fe(CN)_6]^{3-/4-}$. The surface area study is discussed in the Supporting Information.

Fig. 2c illustrates the CV response of different electrodes with or without glucose in 0.1 M NaOH solution. Regardless of whether glucose was added, the anodic current of the bare GCE and MWNTs/GCE remained unchanged, indicating their poor catalytic performance in glucose oxidation. While Cu-MOF/GCE and multilayer films of Cu-MOF/MWNTs/GCE have much higher current in 0.1 M NaOH both with or without glucose. This result further confirmed the effective catalysis

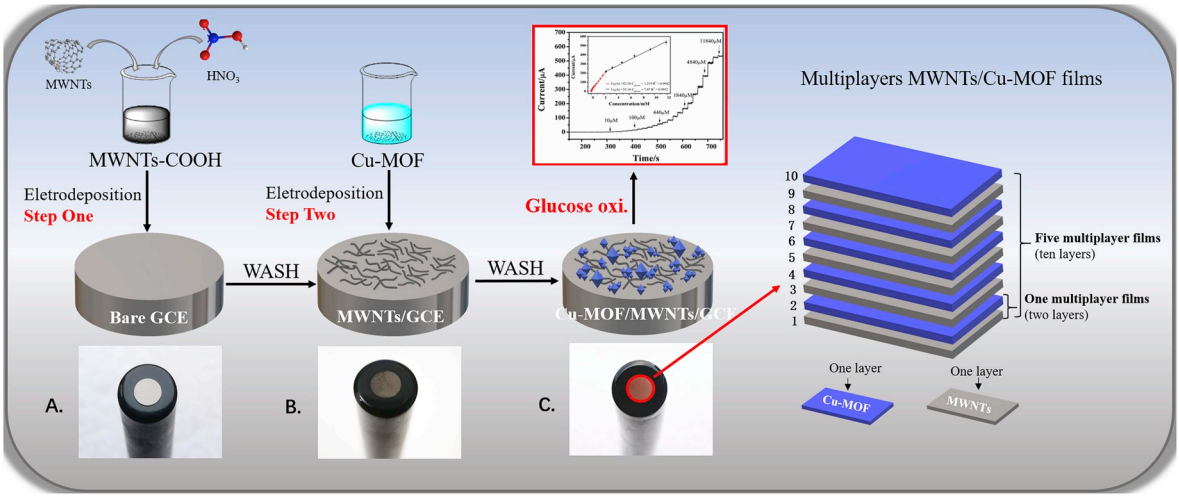

Scheme 1. Schematic illustration of the Cu-MOF and multilayer films of Cu-MOF/MWNTs/GCE.

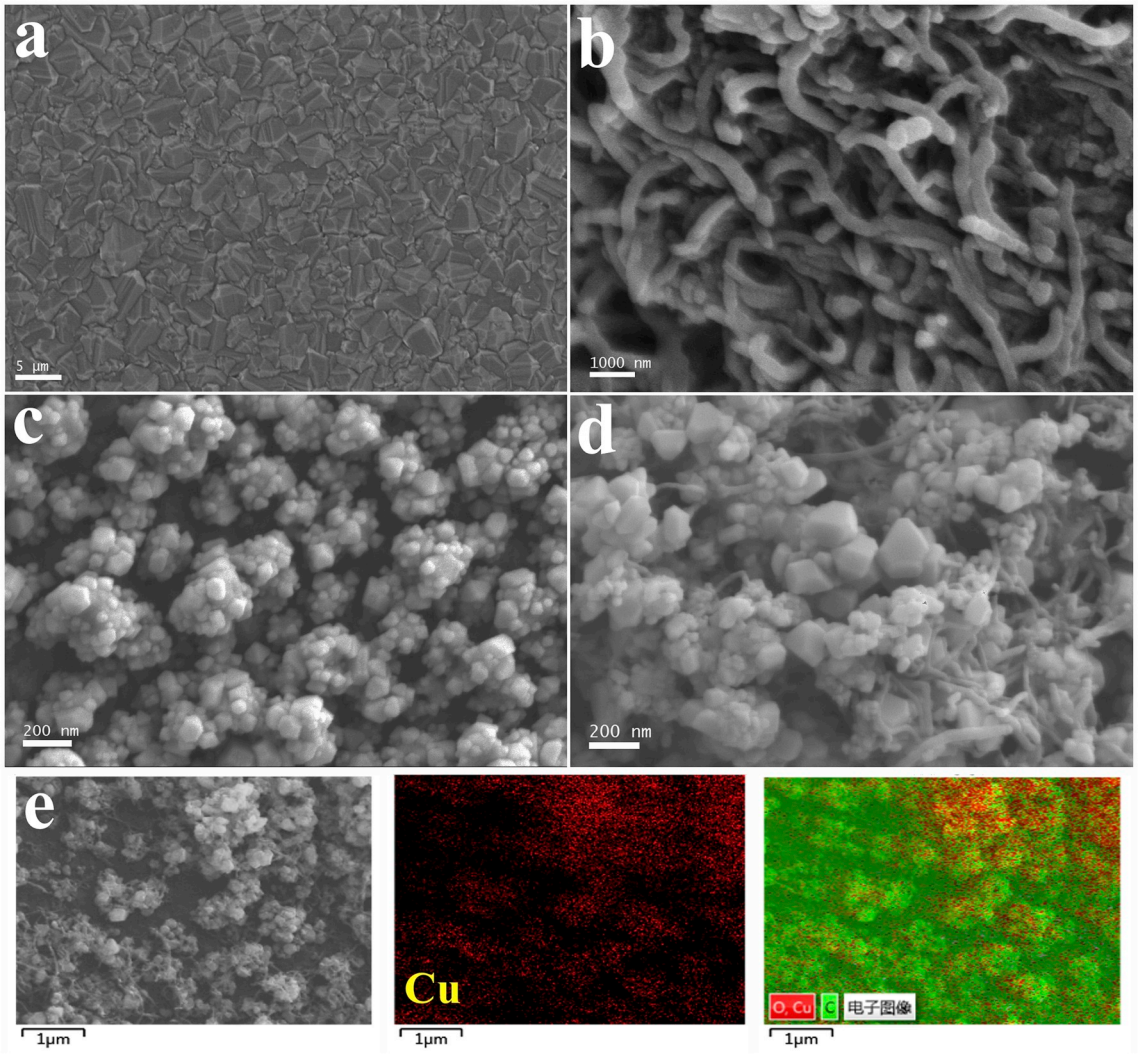

Fig. 1. SEM images of (a) conductive diamond wafer; (b) conductive diamond wafer electrodeposited with MWNTs; (c) conductive diamond wafer electrodeposited with Cu-MOF; (d) conductive diamond wafer electrodeposited with multilayer films of Cu-MOF/MWNTs; and (e) SEM images of Cu-MOF/MWNTs and corresponding elemental mapping of Cu, and O/Cu/C.

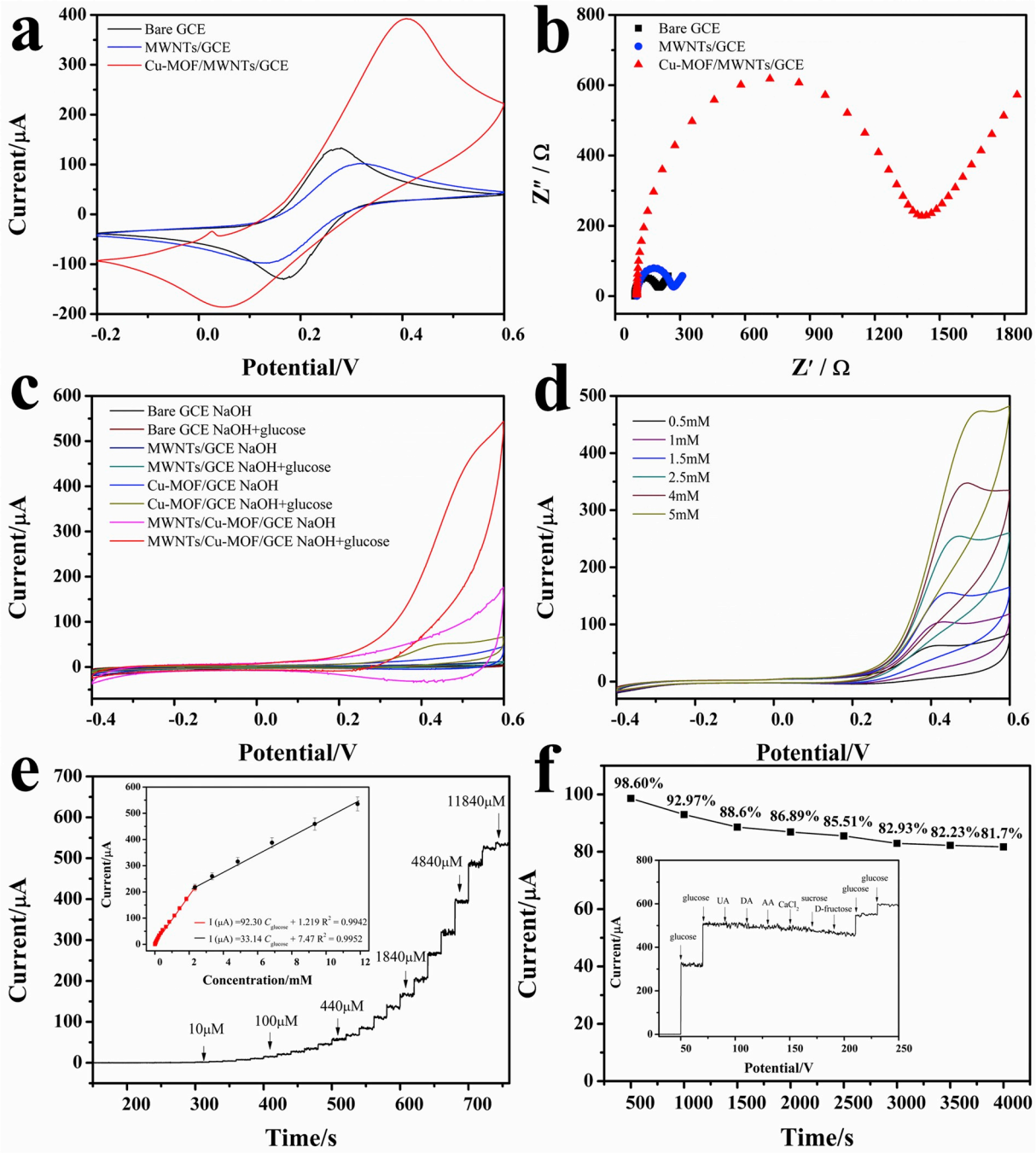

Fig. 2. (a) CV curves and (b) Nyquist plots of EIS (inset shows the fitting equivalent circuit) of bare GCE, MWNTs/GCE and Cu-MOF/MWNTs/GCE in KCl solution containing 5 mM $[Fe(CN)_6]^{3-/4-}$; (c) CV curves of bare GCE, MWNTs/GCE, Cu-MOF/GCE, Cu-MOF/MWNTs/GCE with or without 2.5 mM glucose in 0.1 M NaOH solution; (d) CV curves of Cu-MOF/MWNTs/GCE towards various glucose concentrations in 0.1 M NaOH electrolyte solution; (e) amperometric response of Cu-MOF/MWNTs/GCE to the successive addition of glucose (inset is the corresponding calibration curve); (f) amperometric response curve of multilayer films of Cu-MOF/MWNTs/GCE obtained in the presence of 5 mM glucose at +0.55 V with continuous stirring (inset is the amperometric response of multilayer films of Cu-MOF/MWNTs/GCE to the successive addition of 2.5 mM glucose, 0.25 mM UA, DA, AA, $CaCl_2$, sucrose and D-fructose; 2 mM glucose, 0.25 mM UA, DA, AA, $CaCl_2$, sucrose, and D-fructose; and 2 mM glucose.).

of Cu ion for glucose oxidation, and with the MWNTs can enhance the catalytic effect. This relationship of the anodic peak current versus square root of the scan rate (Fig. S4) indicated that the catalytic oxidation of glucose on the multilayer films Cu-MOF/MWNTs/GCE in 0.1 M NaOH is a diffusion-controlled process (Al-Ahmad et al., 1995; Atta et al., 1996). In addition, the oxidation current significantly increased when the glucose concentration continuously increased from 0.5 mM to 5 mM (Fig. 2d). Therefore, the prepared sensor had a favorable catalytic effect on glucose oxidation. Between 0 V and 0.6 V, the broad oxidation peak current was related to the transition of Cu(I) to Cu (II) and Cu(II) to Cu(III) hydroxide forms. At a potential starting from 0.3 V, the significant oxidation peak current is attributed to Cu(II)–Cu (III) conversion (Shi et al., 2016). The whole catalytic mechanism process of glucose is described as follows:

$$Cu(I)_{MOF} - e^- \leftrightarrow Cu(II)_{MOF} \quad (1)$$

$$Cu(II)_{MOF} + OH^- \leftrightarrow Cu(III)_{MOF} + H_2O + e^- \quad (2)$$

$$Cu(III)_{MOF} + e^- + Glucose \rightarrow Cu(II)_{MOF} + OH^- + Gluconic\ acid \quad (3)$$

3.3. Optimization of preparation and determination conditions

To obtain the best test conditions and achieve the best catalytic effect, we studied the deposition time of the two-step electrodeposition (Figs. S4 and S5). Furthermore, to obtain the quantified determination, +0.55 V was chosen as the optimal potential (Fig. S6). At the optimal potential, amperometry and CV plots of the different layers of multilayer films modified GCE electrode with successive addition of glucose were obtained (Fig. S7). The experiment details are shown in the Supporting Information.

3.4. Sensing performance for glucose detection

The quantitative range of the multilayer films of Cu-MOF/MWNTs/GCE was evaluated by amperometry. The catalytic current of glucose oxidation increased linearly in the concentration range of 0.5 μM–2.34 mM and 2.34 mM–11.84 mM, respectively (Fig. 2e). The calibration plot of the oxidation current *vs.* glucose concentration and the fitting equation are I (μA) = 92.30$C_{glucose}$ (mM) + 1.219 (R^2 = 0.9942) and I (μA) = 33.14$C_{glucose}$ (mM) + 7.47 (R^2 = 0.9952). A sensitivity of 3878 μA cm^{-2} mM^{-1} and a detection limit of 0.4 μM (based on S/N = 3) with a fast response time within 0.3 s were obtained. The sensing performance of the proposed glucose sensor was compared to a series of reported catalysts in Table S1. Of these catalysts, the multilayer films of Cu-MOF/MWNTs/GCE showed a wider linear range, lower detection limit, fast response time and higher sensitivity.

3.5. Selectivity, reproducibility and stability of glucose sensor

In glucose determination, the possible biological small molecule interferences such as uric acid (UA), dopamine (DA), L-ascorbic acid (AA), $CaCl_2$, sucrose and D-fructose, in human blood detection need to be considered. As shown in Fig. 2f, multilayer films of Cu-MOF/MWNTs/GCE showed excellent selectivity for glucose; a negligible response to UA, DA, AA, and $CaCl_2$; and a slight response to sucrose and D-fructose. The stability test showed after 4000 s, the oxidation current was 81.7% of the initial value, which confirmed that the multilayer films of Cu-MOF/MWNTs/GCE were relatively stable. And the reproducibility and the stability of the sensor were confirmed by six modified electrodes prepared in the same way (Fig. S9a); the relative standard difference (RSD) of 4.91% was obtained in response to the successive addition of glucose and the repeatability of the same sensor for nine measurements under the same condition was 7.2% (Fig. S9b).

3.6. Sensor performance for real sample

We verify the detection efficiency of the sensor in real blood samples, by utilizing human serum isolated and obtained from the hospital of the university; the standard addition method was applied (Table S2). The results showed that using the prepared sensor to measure glucose in human blood is feasible and accurate.

4. Conclusions

In sum, a novel method based on constant potential electrodeposition for depositing carboxylated MWNTs and Cu-MOF layer by layer is proposed for the preparation of multilayer composite films non-enzymatic glucose sensor. The multilayer films of Cu-MOF/MWNTs composite material showed an extremely high catalytic effect on glucose catalysis due to the large surface area, multiple catalytic active sites, and good selectivity of the Cu-MOF material in combination with the excellent electrical conductivity of multilayer MWNTs. By reusing crystallization solution, the sensor was prepared simply via electrodeposition in solutions for a certain period to obtain a uniformly dense film. However, strong alkaline condition is still a big limitation to the practical application of the proposed sensor. The following work will improve the applicable conditions of the sensor and further improve its long-term stability.

Declaration of interests

The authors declare that they have no known competing financial interests or personal relationships that could have appeared to influence the work reported in this paper.

CRediT authorship contribution statement

Lan Wu: Conceptualization, Data curation, Formal analysis, Investigation, Methodology, Validation, Writing - original draft. **Zhiwei Lu:** Project administration, Conceptualization, Methodology, Writing - review & editing. **Jianshan Ye:** Funding acquisition, Methodology, Writing - review & editing.

Acknowledgments

This work was supported by the National Natural Science Foundation of China (NSFC, No. 21875070), Science and Technology Program of Guangdong Province (No. 2018A050506006), and Guangdong Nature Science Foundation (No. 2017A030312005). We also wish to thank Engineer Qian Liu from Shiyanjia Lab (www.shiyanjia.com) for his help with the XPS analysis.

Appendix A. Supplementary data

Supplementary data to this article can be found online at https://doi.org/10.1016/j.bios.2019.03.064.

References

Al-Ahmad, S., Boje, B., Magull, J., Rauchfuss, T., Zheng, Y., 1995. J. Am. Chem. Soc. 117 (3), 1145–1146.
Ali Khan, I., Badshah, A., Nadeem, M., Haider, N., Nadeem, M., 2014. Int. J. Hydrogen Energy 39 (34), 19609–19620.
Atta, N., Marawi, I., Petticrew, L., Zimmer, K.H., Mark, B., Galal, H.A., 1996. J. Electroanal. Chem. 408 (1–2), 47–52.
Chowdhury, P., Bikkina, C., Meister, D., Dreisbach, F., Gumma, S., 2009. Microporous Mesoporous Mater. 117 (1–2), 406–413.
Biemmi, E., Scherb, C., Bein, T., 2007. J. Am. Chem. Soc. 129 (26), 8054–8055.
He, J., Yang, H., Zhang, Y., Yu, J., Miao, L., Song, Y., Wang, L., 2016. Sci. Rep. 6, 36637.
Ji, L., Wang, J., Wu, K., Yang, N., 2018. 28, 1706961.
Kang, S.M., Hwang, N.S., Yeom, J., Park, S.Y., Messersmith, P.B., Choi, I.S., Langer, R., Anderson, D.G., Lee, H., 2012. Adv. Funct. Mater. 22 (14), 2949–2955.
Kim, D., Yun, J., Lee, G., Ha, J.S., 2014. Nanoscale 6 (20), 12034–12041.
Liu, F., He, J., Zeng, M., Hao, J., Guo, Q., Song, Y., Wang, L., 2016. J. Nanoparticle Res. 18 (5).
Luo, M., Epps, T.H., 2013. Macromolecules 46 (19), 7567–7579.
Maruyama, T., 1998. Sol. Energy Mater. Sol. Cells 56 (1), 85–92.
Morris, W., Volosskiy, B., Demir, S., Gándara, F., McGrier, P.L., Furukawa, H., Cascio, D., Stoddart, J.F., Yaghi, O.M., 2012a. Inorg. Chem. 51 (12), 6443–6445.
Morris, W., Volosskiy, B., Demir, S., Gándara, F., McGrier, P.L., Furukawa, H., Cascio, D., Stoddart, J.F., Yaghi, O.M., 2012b. Inorg. Chem. 51 (12), 6443–6445.
Okpalugo, T.I.T., Papakonstantinou, P., Murphy, H., McLaughlin, J., Brown, N., 2005. Carbon 43 (1), 153–161.
Shi, L., Zhu, X., Liu, T., Zhao, H., Lan, M., 2016. Sens. Actuators, B 227, 583–590.
Tranchemontagne, D.J., Mendoza-Cortes, J.L., O'Keeffe, M., Yaghi, O.M., 2009. Chem. Soc. Rev. 38 (5), 1257–1283.
Yun S, K.J., 2009. Sens. Actuators, A 154 (1), 73–78.
Zhou, Y., Li, C., Hao, Y., Ye, B., Xu, M., 2018. Talanta 188, 282–287.